

# Anterior Optic Nerve Blood Flow in Experimental Optic Atrophy

J. Sebag,\* G. T. Feke, F. C. Delori, and J. J. Weiter

**This study attempts to establish whether neurogenic optic atrophy induces changes in anterior optic nerve circulation and to determine how noninvasive techniques of measuring blood flow in vivo compare to microsphere distribution. Five cats underwent unilateral optic nerve transection in the orbital apex and a sham procedure in the contralateral eye. Two to three months later, no abnormalities were detected by fluorescein angiography. Laser Doppler measurements demonstrated a 53% decrease in red blood cell speed through the capillaries of the atrophic optic nerve heads in vivo. Optic disk reflectance measurements of anterior optic nerve blood volume in vivo demonstrated a 51% decrease in the estimated blood volume of the capillaries in atrophic optic nerve heads. Flow was calculated on the basis of these noninvasive measurements and demonstrated an average decrease of 74% in optic atrophy. Histologic studies of microsphere distribution demonstrated an average decrease of 80% in flow to the anterior optic nerve in optic atrophy. These results suggest that anterior optic nerve blood flow is significantly reduced in primary neurogenic optic atrophy. This study also demonstrates that the noninvasive measurements of blood flow are substantiated by histologic evaluation of microsphere distribution. Invest Ophthalmol Vis Sci 26:1415-1422, 1985**

Optic nerve atrophy, the sequela of a variety of optic neuropathies, clinically manifests as optic disk pallor. Previously it was believed that this pallor resulted from loss of disk vasculature.<sup>1,2</sup> Recent histologic,<sup>3</sup> ultrastructural,<sup>4</sup> and angiographic<sup>5</sup> studies have shown no substantial loss of capillaries in the pale optic disk. However, in experimental optic atrophy, Quigley found more than a 50% decrease in total tissue volume, while the ratio of capillary number to tissue volume was unchanged.<sup>6</sup> There was also a 27% decrease in the cross-sectional area of the remaining capillaries. Quigley concluded that the changes in vasculature were secondary to nerve fiber loss. On the basis of these findings, one would expect a decrease in total anterior optic nerve capillary blood volume and a slowing in the speed of blood flow. Furthermore, such changes could reflect the extent of nerve fiber degeneration.

There is currently no accurate means of detecting changes in optic nerve circulation in vivo. This becomes important when one considers the findings of Quigley and Green that 20-30% loss of optic nerve

fibers can occur and not be detected clinically by current methods of examination and visual field testing.<sup>7,8</sup> If, as suggested by Quigley, neuronal degeneration induces secondary circulatory changes, the ability to detect subtle changes in anterior optic nerve blood flow in vivo may enable the diagnosis of early optic nerve fiber damage.

This investigation used noninvasive techniques of measuring red blood cell speed (laser Doppler) and blood volume (reflectometry) in the anterior optic nerve capillaries to determine whether optic atrophy induces changes in blood flow. The results obtained in vivo were compared to the results of microsphere distribution in order to evaluate the accuracy and reliability of the noninvasive techniques.

## Materials and Methods

### Animal Model of Optic Atrophy

Five domestic cats weighing 2-3 kg were used in the study and were handled in accordance with the ARVO Resolution on the Use of Animals in Research. General anesthesia was induced by intramuscular injection of 10 mg/kg ketamine and 0.2 mg/kg ace promazine, followed by intravenous boluses of pentobarbital, up to a total of 60 mg. Both optic nerves were exposed via two sagittal incisions in the soft palate and isolated by blunt dissection, as previously described.<sup>9</sup> In each cat, one optic nerve was transected in the orbital apex without bleeding, and the optic nerve of the fellow eye was exposed but not transected. The palate incisions

---

From the Eye Research Institute of Retina Foundation, Boston, Massachusetts.

Presented in part at the Association for Research in Vision and Ophthalmology, Sarasota, Florida, April 1984, and The World Meeting of Neuro-Ophthalmology, Antwerp, Belgium, May 1984.

\* Formerly a Fellow of the Heed Ophthalmic Foundation, 1984-85.

Submitted for publication: February 27, 1985.

Reprint requests: Library, Eye Research Institute, 20 Staniford Street, Boston, MA 02114.

were sutured and intramuscular antibiotics were administered. The cats were examined 2–3 mo later, at which time color disk photography, fluorescein angiography, laser Doppler velocimetry, and reflectometry were performed.

### Laser Doppler Technique

*Theoretical considerations:* The technique is based upon the Doppler effect: laser light that is scattered from a moving particle is shifted in frequency ( $f$ ) by an amount

$$\Delta f = \frac{1}{2\pi} (\vec{K}_s - \vec{K}_i) \cdot \vec{V} \quad (1)$$

where  $\vec{V}$  is the velocity vector of the particle, and  $\vec{K}_i$  and  $\vec{K}_s$  are, respectively, the wavevectors of the incident and scattered light. The magnitudes of the wavevectors are  $2\pi/\lambda$ , where  $\lambda$  is the wavelength of the laser light in the scattering medium. When a region of tissue perfused by capillaries is illuminated by laser light, the superposition of the light scattered by red cells of different velocities and at different angles causes a broadening of the frequency spectrum of the backscattered light. In addition, in tissues such as the anterior optic nerve where the density of capillaries is low, there is a dominant component of the light that has been backscattered by nonvascular elements of the optic nerve.

A theory predicting the shape of the Doppler-broadened frequency spectrum was developed by Stern and Lappe,<sup>10</sup> who applied a "wandering photon" model to the scattering process. In this model, incident laser light diffuses through the tissue, becoming randomly scattered by nonvascular elements. This randomness eliminates any directionality to the incident light. Furthermore, this randomized scattering by nonvascular tissue will not induce any shift in the frequency spectrum of reflected light. Only moving red blood cells can induce such a shift.

The frequency shift spectrum  $S(\Delta f)$  of the backscattered light is composed of a series of components each corresponding to light that has been sequentially scattered by  $n$  different moving red cells. The first order component ( $n = 1$ ) dominates the total spectrum at low frequencies.<sup>10</sup> Furthermore, the first order spectrum varies as the negative logarithm of  $\Delta f$  at low frequencies:  $-\log(\Delta f)$ . This logarithmic variation will occur for any velocity distribution that may be present. At higher frequencies, due to the effects of multiple scattering and the anisotropic scattering by red cells, there is a "tail" that gradually approaches zero amplitude.

The low frequency portion of  $S(\Delta f)$  can be expressed as

$$S(\Delta f) = -K \log(\Delta f/\alpha) \quad (2)$$

where  $K$  is a measure of the spectrum's amplitude and the frequency  $\alpha$  is a measure of the spectrum's broadening, which is proportional to the red cell speeds that are present.

For an idealized case of a random array of blood vessels each carrying red cells having a constant velocity distribution up to a maximum value,  $V_{\max}$ , and for isotropic scattering by the red cells, Stern and Lappe<sup>10</sup> show that

$$\alpha = 2 V_{\max}/\lambda. \quad (3)$$

This idealized formula provides an estimate of the actual red blood cell speeds that can be expressed in mm/sec by the equation

$$V_{\max}(\text{mm/sec}) = \alpha(H_z) \cdot 2.38 \times 10^{-4}. \quad (4)$$

More importantly, however, measurement of the frequency parameter  $\alpha$  provides a consistent, generally applicable means to characterize the speed of red blood cells flowing in the capillaries of the anterior optic nerve.

*Data acquisition:* Anesthesia was induced as described above. Phenylephrine 10% was instilled in both eyes to retract the nictitating membrane, and mydriacyl was used to maximize pupillary dilatation. The cats were positioned prone before a fundus camera apparatus equipped with a helium–neon laser light source and a scanning fiberoptic-photomultiplier detector assembly that collects the scattered light.<sup>11,12</sup> The incident laser beam was directed into the eye and positioned onto the optic disk. Examination with red-free light enabled the identification of vessels on the disk surface, which were avoided to ensure that measurements were obtained from regions of disk tissue perfused by capillaries.

Measurement sites were approximately 140  $\mu\text{m}$  in diameter, as determined by the fiberoptic entrance aperture, the camera magnification, and the dioptric power of the reduced schematic eye for the cat.<sup>13</sup> The photocurrent signal from the detector was recorded continuously on a Honeywell 5600 C Recorder/Reproducer (Honeywell, Inc.; Newton, MA) for approximately 1 min. The mean value of the photocurrent, a measure of the intensity of the scattered light, was continuously displayed on a strip chart recorder.

The photocurrent signal was also channelled through a loudspeaker. The audio signal from the disk tissue is easily distinguished from that of an individual vessel and is a useful guide in maintaining the position of the incident beam during the measurement.

*Data analysis:* The portion of tape recorded during optimal conditions of eye stability, incident beam alignment, and detector alignment is identified by examining the continuous recording of the mean photocurrent. The frequency spectrum of the photocurrent

is then obtained using a Federal Scientific UA 500 (Federal Scientific Corp.; NY, NY) ubiquitous real time spectrum analyzer. Spectra were obtained using a 2-kHz full scale range with an averaging time of 8 sec. The results were recorded on an X-Y plotter. Amplitude and log frequency data in the range 30–200 Hz at 10 Hz intervals were entered into a computer. All spectra were fit either to the single logarithmic form predicted by the theory or to the sum of two logarithmic curves (see Results).

### Optic Disk Reflectometry

*Theoretical considerations:* Spectral reflectometry of the optic disk was used in this study to quantify the degree of disk "pallor" and to estimate, in vivo, the amount of blood present in the tissue of the optic nerve head. Determination of the amount of blood in tissues through interpretation of reflectance measurements requires understanding of the optical propagation through both the surrounding bloodless tissue and the blood, as well as an appropriate mathematical description of the relation between reflectance, amount of blood, and scattering characteristics of the tissue. Theoretical approaches to this problem based on the Kubelka-Monk theory<sup>14</sup> and on multiple scattering and photon diffusion theories<sup>15</sup> have been suggested. However, these methods are not easily applicable, require absolute reflectance measurements, and require knowledge of the scattering properties of the tissue, distribution of the blood in the tissue, and size of both the illumination and detection areas on the tissue during reflectance measurement.

Because the volume fraction of blood in the tissues of the optic nerve head is small, about 2%,<sup>16</sup> one can assume that the reflectance  $R_\lambda$  at a wavelength  $\lambda$  is given by

$$R_\lambda = T_\lambda^2 \cdot R'_\lambda \cdot [1 - \gamma \cdot K_\lambda] \quad (5)$$

where  $T_\lambda$  is the transmission of the ocular media,  $\gamma$  is a measure for the amount of blood (cm),  $K_\lambda$  is the known absorption coefficient of hemoglobin (1/cm), and  $R'_\lambda$  the bloodless ( $\gamma = 0$ ) reflectance of the disk. Equation (5) must be considered as a first degree approximation of any of the abovementioned theoretical approaches, valid only if the quantity  $\gamma$  is very small. This relationship, with  $T_\lambda = 1$ , can for example be deduced from the Kubelka-Monk reflectance equation for thick layers of intensively scattering tissue,<sup>14</sup> in the assumption that the volume fraction of blood  $v$  is very small: the quantity  $\gamma$  is then proportional to  $v$  but inversely proportional to the scattering coefficient of the tissue. The determination of  $\gamma$  therefore does not allow, a priori, differentiation between changes in blood volume and changes in the scattering properties of the tissue. It should also be noted that the value of  $\gamma$  can

be interpreted as the thickness of an equivalent thin layer of blood located in front of a bloodless disk.

The measurement of  $R_\lambda$ , the absolute reflectance of the disk, is difficult to perform with accuracy by fundus reflectometry because of uncertainties in the transmission of the ocular media, possible obstruction of illumination beam by the pupil, and complications in referencing the disk measurements with those of an absolute reflectance standard placed in an artificial eye with matching focal length. These difficulties are alleviated or eliminated by performing measurement of relative reflectances at different wavelengths in rapid succession, and by defining reflectance ratios:

$$r_\lambda = \frac{R_\lambda}{R_{\lambda_0}} \quad (6)$$

where  $\lambda_0$  is a reference wavelength.

The bloodless reflectance of the disk and the transmission,  $T_\lambda$ , cannot a priori be considered to be wavelength independent. For the narrow spectral range (550–600 nm) in which reflectance measurements are made, we have furthermore assumed that the following linear approximation is valid:

$$R'_\lambda \cdot T_\lambda^2 = R'_{\lambda_0} \cdot T_{\lambda_0}^2 [1 + \beta(\lambda - \lambda_0)] \quad (7)$$

where  $\beta$  is an unknown factor and  $\lambda_0$  the reference wavelength. Substitution of equations (5) and (7) in equation (6) gives:

$$r_\lambda = [1 + \beta(\lambda - \lambda_0)] \cdot \frac{1 - \gamma K_\lambda}{1 - \gamma K_{\lambda_0}} \quad (8)$$

The unknowns  $\gamma$  and  $\beta$  can be solved from two relationships such as equation (8), but with  $\lambda = \lambda_1$  and  $\lambda = \lambda_2$ . Using the common reference wavelength  $\lambda_0$  this represents measurements at three wavelengths.

*Data acquisition:* Reflectance measurements at three wavelengths were obtained from the central area of the optic disk using the Retinal Vessel Oximeter instrument<sup>17</sup> operated in its reflectometry mode. The fundus was illuminated over an area of about 5 deg successively at three wavelengths  $\lambda_0 = 569$ ,  $\lambda_1 = 559$ , and  $\lambda_2 = 585$  nm, and the light reflected from a  $250 \times 250 \mu\text{m}$  area of the cat's optic disk was detected. Microcomputer control of the instrument allows signal averaging, and the calculation, every 3 sec, of the intensity of the reflected light signal at the three wavelengths. Typically, about 20 such 3-sec measurements were made and averaged for each optic disk. Measurement of light intensities reflected from a magnesium oxide reflectance standard allows correction of the disk data to account for differences in the illumination intensities and detection sensitivities at the three wavelengths. The results then represent the ratios:

$$r_1 = R(559)/R(569) \text{ and } r_2 = R(585)/R(569)$$

with  $R(\lambda)$  being the measured reflectance of the disk at a wavelength  $\lambda$ .

**Data analysis:** The measured ratios  $r_1$  and  $r_2$  generate two equations similar to equation (8) with  $\lambda_0 = 569$  and  $\lambda_1 = 559$ , or  $\lambda_2 = 585$  nm. These equations can be solved by eliminating  $\beta$ , to yield:

$$\gamma = \frac{w(r_1 - 1) - r_2 + 1}{K_0(w \cdot r_1 - r_2) - K_1 \cdot w + K_2} \quad (9)$$

where  $w = (585 - 569/559 - 569)$ . Oxygen saturation of the blood in the disk capillaries was assumed to be 80%, yielding values of  $K_0 = 174$ ,  $K_1 = 148$ , and  $K_2 = 113 \text{ cm}^{-1}$ , respectively, for the wavelengths 569, 559, and 585 nm. Hemoglobin concentration of cat blood was assumed to be 11 g/100 ml,<sup>18</sup> and extinction coefficients given by Van Assendelph<sup>19</sup> were used. The resulting values of  $\gamma$  depend somewhat upon the assumed value of 80% saturation: a decrease of about 20% in the value of  $\gamma$  is calculated when the assumed saturation increases from 70 to 90%. However, this dependence affects measurements on all disks similarly, such that the ratio of the  $\gamma$  values for atrophic and normal disks are not critically affected (less than 1% change) if the saturation in both disks is the same.

### Microsphere Distribution Studies

Histologic studies of microsphere distribution to the anterior optic nerve were performed after all in vivo investigations were completed. Anesthesia was induced as described above. A thoracotomy was performed and 2.0 ml of a suspension of black, nonlabeled microspheres ( $9 \pm 1 \mu\text{m}$ , 3M Company; St. Paul, MN) in 10% dextran (0.5 g/ml) was injected into the left ventricle, followed by an intraventricular injection of 2.0 ml of 5% KCl, causing instantaneous death.

Both eyes were enucleated and the optic nerve and surrounding tissues of the posterior pole to about the equator were excised en bloc. The tissues were stored in formalin, processed by hand through ethanol of increasing concentration, xylene, and paraffin, and then embedded in paraffin. The entire thickness of the optic nerve was cut longitudinally along with surrounding tissues in 8- $\mu\text{m}$  thick sections and mounted on glass slides. Paraffin was removed with xylene, and coverslips were placed using immersion oil. Hematoxylin and eosin were used to stain selected slides.

A Zeiss Photomicroscope III (Carl Zeiss; Oberkochen, West Germany) was used to examine the slides and count microspheres in the prelaminar, laminar, and first 400- $\mu\text{m}$  portion of the retrolaminar optic nerve. In addition, 400- $\mu\text{m}$  wide sections of full-thickness neural retina and choroid/tapetum were examined in approximately the same locations for each pair of eyes. Clumps of microspheres were considered as one

microsphere. Microspheres that were transected during cutting and objects that appeared smaller, lighter in color, or with irregular edges were not counted. The number of microspheres in each tissue compartment of every section in all eyes were tabulated, normalized to the counts obtained in the choroid/tapetum, and the results evaluated using the parametric paired two-tailed t-test.

### Results

All cats demonstrated a total afferent pupillary defect in the eye that underwent optic nerve transection. Fundus examination revealed no vascular abnormalities. Fluorescein angiography demonstrated normal filling of retinal vessels and no abnormality in choroidal or disk fluorescence (Fig. 1).

### Laser Doppler Measurements

Laser Doppler measurements were obtained from the anterior optic nerves of both eyes of each animal. Figure 2 shows the measurements from one of the animals. The Doppler-broadened frequency spectrum obtained from the normal control optic nerve is shown in the upper left. The spectrum obtained from the atrophic optic nerve is shown in the lower left. To determine the parameter  $\alpha$  which characterizes the broadening of the spectrum, points along the spectrum were plotted as a function of the logarithm of the frequency shift as shown in the upper and lower right of Figure 2. A single linear regression analysis was used to fit each spectrum from normal control optic nerves. As shown in Figure 2 upper right, the broadening parameter  $\alpha$  is specified by the frequency at which the linear fit intersects the abscissa. The logarithmic curve determined by the parameters of the linear fit was plotted and superimposed on the spectrum as shown in the upper left of Figure 2.

A single linear regression analysis could not be used to fit any of the spectra from atrophic optic nerves. When points along each of these spectra were plotted as a function of the logarithm of the frequency shift, the results were similar to the example shown in the lower right of Figure 2. These points were well fit by the sum of two straight lines, one intersecting the abscissa at  $\alpha_1$ , and the other intersecting the abscissa at  $\alpha_2$ . In addition to determining  $\alpha_1$  and  $\alpha_2$  for each of the atrophic optic nerves, a mean broadening parameter,  $\bar{\alpha}$ , was calculated as a weighted average of  $\alpha_1$  and  $\alpha_2$  in each case. The relative weights of  $\alpha_1$  and  $\alpha_2$  in calculating  $\bar{\alpha}$  were determined by the relative areas under the two logarithmic curves corresponding to  $\alpha_1$  and  $\alpha_2$ .

Table 1 shows the laser Doppler results obtained from each of the cats. As shown in Table 1, both  $\alpha_1$  and  $\alpha_2$  in the atrophic optic nerve of each cat were



Fig. 1. Fluorescein angiography of cat eye 10 wk after optic nerve transection. Retinal vessels filled normally and no disk or choroidal filling defects were observed. *Left*, Early arteriovenous phase; *right*, late A-V phase.

lower than the  $\alpha$  determined for the contralateral normal control optic nerve. Table 1 also shows that there was an average reduction of 53% in red blood cell speed

in the atrophic optic nerves compared to the contralateral normal optic nerves ( $P < 0.01$ ).

One cat (#1) was examined at 1 and 3 mo following

Fig. 2. Laser Doppler measurements of anterior optic nerve blood flow. The Doppler-broadened frequency shift spectrum in the normal optic nerve (*upper left*) is broader than in the atrophic optic nerve (*lower left*). The semilogarithmic representations of these data demonstrate a single logarithmic fit in the normal eye (*upper right*). The data from the eye with optic atrophy are best fit by the sum of two logarithmic functions (*lower right*). Alpha ( $\alpha$ ) is the point of intersection with the abscissa and is directly proportional to  $V_{max}$  (equation 4). Both alpha values in the atrophic optic nerve are substantially lower than in the normal optic nerve, representing a decrease in the speed of blood flow.

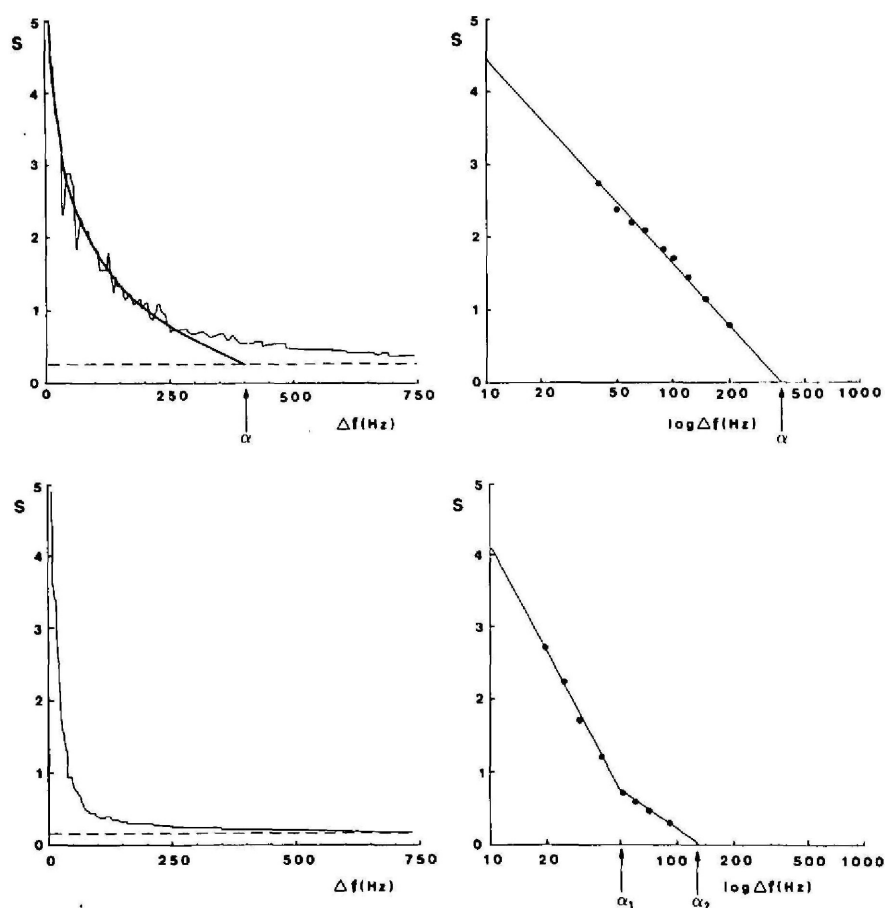


**Table 1.** Results of laser Doppler measurements

Cat no.	$\alpha^*$ (Normal)	$\alpha_1$ (Atrophic)	$\alpha_2$ (Atrophic)	$\bar{\alpha}$ (Mean)	$\bar{\alpha}/\alpha$ (Atrophic/normal)
1	282	65	224	213	0.76
2	316	40	138	100	0.32
3	390	52	148	120	0.31
4	282	50	162	108	0.38
5	437	117	331	261	0.60
Mean	314 (69)†	65 (31)	201 (80)	160 (72)†	0.47 (0.20)

\* Alpha ( $\alpha$ ) is the index of red blood cell speed through the capillaries of the anterior optic nerve and is expressed as Hz. Numbers in parentheses are standard

deviations.

†  $P < 0.01$ .

unilateral optic nerve transection. In the control eyes, the same  $\alpha$  value (282 Hz) was obtained on each occasion. In the eye with optic atrophy the  $\bar{\alpha}$  at 1 mo was 198 Hz and at 3 mo,  $\bar{\alpha}$  was 213 Hz, indicating no significant change in the speed of blood flow during the second and third months following optic nerve transection.

#### Optic Disk Reflectometry Measurements

Table 2 gives the results for the reflectance ratios  $r_1$  and  $r_2$  for the normal and atrophic disks in the five cats. Standard deviations in these ratios ranged between 0.1% and 0.47% (average, 0.3%). A statistically significant decrease in the ratio  $r_2$  was found for all 5 cats between the atrophic and the normal disks  $P < 0.001$ . The values of  $\gamma$  were calculated using equation (9), for each of the  $r_1 - r_2$  ratio pairs and the results are shown in Table 2, along with the standard deviations in  $\gamma$  (calculated by error propagation in each case). The variability in the measure  $\gamma$  increases with decreasing values of  $\gamma$ , and the measurements become inaccurate for low values of  $\gamma$ . The values of  $\beta$ , derived in the solution of equations (4) to (8) ranged between  $-7 \times 10^{-4}$  and  $+20 \times 10^{-4} \text{ nm}^{-1}$ . The values of  $\gamma$  were significantly different for all cats at the  $P < 0.001$  level, except for cat 5. Table 2 also gives the ratios of  $\gamma$  between the atrophic and normal disks.

#### Noninvasive Blood Flow Calculations

Relative changes in blood flow through the capillaries of the anterior optic nerve can be calculated by using the laser Doppler index of red blood cell speed and the

reflectance estimate of relative blood volume under the abovementioned assumptions. The ratio  $F$  between blood flows in the atrophic to the normal disks is then:

$$F(\text{atrophic/normal}) = \frac{\bar{\alpha}_{\text{atrophic}}}{\alpha_{\text{normal}}} \cdot \frac{\gamma_{\text{atrophic}}}{\gamma_{\text{normal}}} \quad (10)$$

where  $\alpha$  = index of average speed of red blood cells in normal optic nerves as measured by the laser Doppler technique, and where  $\gamma$  = the ratio of blood volume to tissue scattering as measured by reflectometry. The results of these calculations are shown in Table 3, and demonstrate that as measured by noninvasive techniques, blood flow was reduced in atrophic optic nerve heads by an average of 74%.

#### Histologic Studies of Microsphere Distribution

The intracardiac injection of microspheres was successful in four of the five cats. Substantially more microspheres were found in the choroid than in other tissues, consistent with the greater blood flow to this tissue. There was no significant difference between the number of microspheres in the choroid/tapetum of eyes with optic atrophy as compared to control eyes. There were, however, significantly fewer microspheres in atrophic optic nerves than in normal controls. Table 3 shows these results expressed as the ratio of the number of microspheres in atrophic optic nerves to the number in normals. There was close correlation between the microsphere data and noninvasive measurements in all cats except cat 5.

Comparisons of the means and expected ranges of microsphere counts at the 95% confidence level<sup>20</sup> dem-

**Table 2.** Optic disk reflectometry measurements

Cat no.	Normal			Atrophic			$(\gamma)_{\text{atrophic}}/(\gamma)_{\text{normal}}$
	$r_1$ (%)	$r_2$ (%)	$\gamma (10^{-6})$	$r_1$ (%)	$r_2$ (%)	$\gamma (10^{-6})$	
1	100.36	103.01	329 (50)	101.39	100.13	220* (75)	0.67
2	98.92	103.33	152 (43)	99.87	100.80	57* (40)	0.37
3	98.49	104.73	217 (53)	99.37	101.73	69* (56)	0.32
4	102.63	103.37	654 (71)	100.59	101.81	256* (31)	0.39
5	98.73	102.82	75 (54)	100.29	100.10	54 (52)	0.71
Mean							0.49 (0.18)

\*  $P < 0.001$  between the two optic nerves in each cat. Numbers in parentheses are standard deviations.

onstrated that there was no overlap in the results obtained from the optic nerve and retina of normal eyes as compared to eyes with optic atrophy. Statistical analysis of the means and standard deviations of these counts demonstrated that there were significant differences between the number of microspheres present in the anterior optic nerve and retina of eyes with optic atrophy as compared to controls. Optic nerve microsphere counts were reduced an average of 80% in optic atrophy ( $P = 0.04$ ). Microsphere counts in the neural retina demonstrated that eyes with optic atrophy had 63% fewer microspheres than did controls ( $P = 0.02$ ).

### Discussion

This study demonstrates that there is a significant decrease in blood flow in primary neurogenic optic atrophy that is measurable by noninvasive techniques. An approach for the analysis of laser Doppler measurements obtained from capillary beds in the skin has been previously described.<sup>10</sup> This approach was utilized in previous studies of anterior optic nerve blood flow.<sup>21-23</sup> Using this approach, we have demonstrated a significant decrease in the speed of red blood cells through the capillaries of the anterior optic nerve in primary neurogenic optic atrophy.

Optic disk reflectometry measurements were used to estimate anterior optic nerve blood volume in vivo. These results demonstrated a substantial decrease in capillary blood volume induced by neurogenic optic atrophy. As noted above, differences in scattering properties of the tissues between the atrophic and normal optic disks will influence these measurements. Thus, it could be argued that the presence of gliosis or astrocyte proliferation surrounding the capillaries of an atrophic optic nerve interferes with the incident and/or scattered (reflected) light and results in artifactual measurement of decreased blood volume which would in turn result in the observation of decreased blood flow.

Significant astrocyte proliferation in the monkey begins at 6 wk<sup>4</sup> and is very noticeable in the cat by 8 wk<sup>3</sup> after optic nerve transection. This progression in astrocyte proliferation did not appear to significantly alter the laser Doppler measurements of red blood cell speed in the cat examined at 1 and 3 mo after optic nerve transection. This finding is consistent with the predictions of the "wandering photon" model,<sup>10</sup> where randomness of incident and scattered light is not affected by increases in the scattering properties of tissues surrounding the anterior optic nerve capillaries. Theoretically, increased tissue scattering would decrease the value of  $\gamma$ , since  $\gamma$  is proportional to the ratio of fractional blood volume and the scattering coefficient of the tissue. An increase in tissue scattering could thus result in an overestimation of the decrease in blood

**Table 3.** Comparison of noninvasive and histologic blood flow\* determinations

Cat no.	Non-invasive (atrophic/normal)	Microspheres (atrophic/normal)
1	0.51	0.44
2	0.12	—
3	0.10	0.08
4	0.15	0.16
5	0.43	0.13
Mean	0.26 (0.19)	0.20 (0.16)

\* Flow was calculated for each cat using equation 10 and is expressed as the ratio in the atrophic optic nerve over the normal optic nerve. Numbers in parentheses are standard deviations.

flow as determined by noninvasive techniques. However, the results of the histologic microsphere distribution studies support the results obtained by noninvasive techniques.

Validation studies on the distribution of microspheres in the cat have shown that the right and left hemispheres of the brain obtain similar fractions of microspheres, indicating even mixture and distribution.<sup>24</sup> Physiologic studies have demonstrated that  $9 \pm 1 \mu\text{m}$  microspheres behave like erythrocytes.<sup>25</sup> Anatomic studies showed that these microspheres lodge in vessels with a mean diameter of  $11.5 \pm 3.4 \mu\text{m}$  indicating their ability to perfuse terminal vessels and not lodge at bifurcations, as can occur with larger microspheres.<sup>26</sup> Furthermore,  $9 \pm 1 \mu\text{m}$  microspheres are trapped in the lungs, eliminating any recirculation. The microsphere technique has been successfully used to study the effect of elevated intraocular pressure on retinal and optic nerve blood flow in monkeys,<sup>27</sup> and the effects of topical epinephrine and aphakia on ocular blood flow, including the optic nerve.<sup>28</sup> Nevertheless, a variety of systemic factors, including depth of anesthesia, systemic blood pressure, and cardiac output can affect the distribution of microspheres. Without monitoring these variables, one cannot use the results to derive absolute measurements of blood flow. This approach can, however, be used to accurately determine relative changes in blood flow. Because each cat in this study had a normal eye that underwent a sham procedure without optic nerve transection, any difference between the two eyes is significant since the same systemic factors affect both eyes of each cat. Thus, it is reasonable to conclude that the results obtained by laser Doppler techniques are not attributable to artifact, and that the changes observed by reflectometry could only partially be the result of increased scattering.

The finding that primary neurogenic optic atrophy induces a decrease in blood flow to the anterior optic nerve in vivo is consistent with the histologic findings of Quigley, that there is a decrease in the total number of capillaries in the anterior optic nerve and a 27% decrease in the cross-sectional area of the remaining

capillaries.<sup>6</sup> The finding that optic atrophy induces a decrease in blood flow to the neural retina agrees with the observations of Frisen.<sup>29</sup> Studying the changes in arteriolar diameter caused by descending optic atrophy, Frisen predicted that retinal blood flow would be decreased by 67%. This is supported by our finding of a 63% decrease in blood flow to the neural retina as determined by microsphere studies.

The noninvasive techniques used in this study were able to detect the substantial decrease in blood flow to the anterior optic nerve in vivo. The comparison between these noninvasive techniques and microsphere distribution appears to validate the accuracy of the noninvasive techniques in measuring flow. Further studies are needed to confirm these findings using techniques that are superior to microsphere distribution in assessing actual optic nerve tissue perfusion.<sup>30-32</sup> The refinement of these noninvasive techniques may provide a means of detecting early optic nerve fiber loss and enable therapeutic intervention prior to irreversible visual loss in such diseases as glaucoma.

**Key words:** optic nerve, optic atrophy, blood flow, laser Doppler, reflectometry, microspheres

### Acknowledgments

Dr. Harry A. Quigley kindly reviewed the manuscript. Outstanding technical assistance was provided by Karlotta Fitch, Douglas Goger, and Virginia Flook.

### References

- Cogan DG: Neurology of the Visual System. Springfield, Charles C. Thomas, 1966, p. 133.
- Walsh FG and Hoyt WF: Clinical Neuroophthalmology, 3rd ed. Baltimore, Williams and Wilkins, 1969, p. 635.
- Henkind P, Bellhorn R, Rabkin M, and Murphy ME: Optic nerve transection in cats. II. Effect on vessels of optic nerve head and lamina cribrosa. *Invest Ophthalmol Vis Sci* 16:442, 1977.
- Quigley HA and Anderson DR: The histologic basis of optic disk pallor in experimental optic atrophy. *Am J Ophthalmol* 83:709, 1977.
- Radius RL and Anderson DR: The mechanism of disc pallor in experimental optic atrophy: A fluorescein angiographic study. *Arch Ophthalmol* 97:532, 1979.
- Quigley HA, Hohman RM, and Addicks EM: Quantitative study of optic nerve head capillaries in experimental optic disk pallor. *Am J Ophthalmol* 93:689, 1982.
- Quigley HA and Green WR: The histology of human glaucoma cupping and optic nerve damage: clinicopathologic correlation in 21 eyes. *Ophthalmology* 86:1803, 1979.
- Quigley HA, Addicks EM, Green WR, and Maumenee AE: Optic nerve damage in human glaucoma. II. The site of injury and susceptibility to damage. *Arch Ophthalmol* 99:635, 1981.
- Henkind P, Gould HB, and Bellhorn RW: Optic nerve transection in cats: effect on retinal vessels. *Invest Ophthalmol* 14:610, 1975.
- Stern MD and Lappe DL: Method and apparatus for measurement of blood flow using coherent light. U.S. Patent No. 4,109,647; 1978.
- Feke GT and Riva CE: Laser Doppler measurements of blood velocity in human retinal vessels. *J Opt Soc Am* 68:526, 1978.
- Green GJ, Feke GT, Goger DG, and McMeel JW: Clinical application of the laser Doppler technique for retinal blood flow studies. *Arch Ophthalmol* 101:971, 1983.
- Hughes A: A useful table of reduced schematic eyes for vertebrates which includes computed longitudinal chromatic aberrations. *Vision Res* 19:1273, 1979.
- Kubelka P: New contributions to the optics of intensely light-scattering materials. *J Opt Soc Am* 38:448, 1948.
- Takatani S: On the theory and development of a noninvasive tissue reflectance oximeter. Thesis, Case Western Reserve University, 1978.
- Quigley HA, Hohman RM, Addicks EM, and Green WR: Blood vessels of the glaucomatous optic disc in experimental primate and human eyes. *Invest Ophthalmol Vis Sci* 25:918, 1984.
- Delori FC, Rogers FJ, Bursell SE, and Parker JS: A system for non-invasive oximetry of retinal vessels. In *Frontiers of Engineering in Health Care-1982*, Potvin AR and Potvin JH, editors. New York, Institute of Electrical and Electronics Engineers, 1982, pp. 296-299.
- Altman PL and Dittmer DS: Erythrocyte and hemoglobin values in vertebrates. In *Biology Data Book*, Vol III, Bethesda, Maryland, Federation of American Societies for Experimental Biology, 1974, p. 1851.
- Van Assendelft OW: Spectrophotometry of Hemoglobin Derivatives. Springfield, Charles C. Thomas, 1970.
- Buckberg GD, Luck JC, Payne DB, Hoffman JIE, Archie JP, and Fixler DE: Some sources of error in measuring regional blood flow with radioactive microspheres. *J Appl Physiol* 31:598, 1971.
- Riva CE, Feke GT, and Loebl M: Blood flow in the capillaries of the optic nerve. In *Proceedings of the 5th Congress of the European Society of Ophthalmology*, Francois J editor, Hamburg, 1976. Stuttgart, Ferdinand Enke Verlag, 1978, pp. 414-416.
- Riva CE, Grunwald JE, and Sinclair SH: Laser Doppler measurement of relative blood velocity in the human optic nerve head. *Invest Ophthalmol Vis Sci* 22:241, 1982.
- Sebag J, Bienfang DC, Feke GT, and Weiter JJ: Unilateral optic disc swelling associated with acute elevation of intraocular pressure. Session X, Fourth Meeting of the International Society of Neuroophthalmology, Hamilton, Bermuda, 1982.
- Hof RP, Wyler F, and Stadler G: Validation studies for the use of the microsphere method in cats and young minipigs. *Basic Res Cardiol* 75:747, 1980.
- Phibbs RH and Dong L: Nonuniform distribution of microspheres in blood flowing through a medium-size artery. *Can J Physiol Pharmacol* 48:415, 1970.
- Dickhoner WH, Bradley BR, and Harell GS: Diameter of arterial microvessels trapping 8-10 micron, 15 micron and 25 micron microspheres as determined by vital microscopy of the hamster cheek pouch. *Invest Radiol* 13:313, 1978.
- Geijer C and Bill A: Effects of raised intraocular pressure on retinal, prelaminar, laminar, and retrolaminar optic nerve blood flow in monkeys. *Invest Ophthalmol Vis Sci* 18:1030, 1979.
- Caprioli J, Sears M, and Mead A: Ocular blood flow in phakic and aphakic monkey eyes. *Exp Eye Res* 39:1, 1984.
- Frisén L and Claesson M: Narrowing of retinal arterioles in descending optic atrophy: a quantitative clinical study. *Ophthalmology* 91:1342, 1984.
- Sossi N and Anderson DR: Effect of elevated intraocular pressure on blood flow. Occurrence in cat optic nerve head studied with Iodoantipyrine I 125. *Arch Ophthalmol* 101:98, 1983.
- Weinstein JM, Duckrow RB, Beard D, and Brennan RW: Regional optic nerve blood flow and its autoregulation. *Invest Ophthalmol Vis Sci* 24:1559, 1983.
- Hohman RM, Addicks EM, and Quigley HA: Optic nerve and retinal blood flow measurement in experimental glaucoma using tritiated iodoantipyrine. ARVO Abstracts. *Invest Ophthalmol Vis Sci* 24(Suppl):102, 1983.